

Formation of apoptosome is initiated by cytochrome *c*-induced dATP hydrolysis and subsequent nucleotide exchange on Apaf-1

Hyun-Eui Kim, Fenghe Du, Min Fang, and Xiaodong Wang*

Howard Hughes Medical Institute and Department of Biochemistry, University of Texas Southwestern Medical Center, Dallas, TX 75390

This contribution is part of the special series of Inaugural Articles by members of the National Academy of Sciences elected on April 20, 2004.

Contributed by Xiaodong Wang, September 13, 2005

Apoptosis in metazoans is executed by a group of intracellular proteases named caspases. One of the caspase-activating pathways in mammals is initiated by the release of cytochrome *c* from mitochondria to cytosol, where it binds to Apaf-1 to form a procaspase-9-activating heptameric protein complex named apoptosome. We report here the reconstitution of this pathway with purified recombinant Apaf-1, procaspase-9, procaspase-3, and cytochrome *c* from horse heart. Apaf-1 contains a dATP as a cofactor. Cytochrome *c* binding to Apaf-1 induces hydrolysis of dATP to dADP, which is subsequently replaced by exogenous dATP. The dATP hydrolysis and exchange on Apaf-1 are two required steps for apoptosome formation.

apoptosis | mitochondria | caspase | dATPase

The characteristic morphological and biochemical markers of apoptotic cell death can be attributed to the activity of a group of intracellular proteins, caspases (1). These markers include DNA cleavage into nucleosomal fragments, chromatin aggregation, membrane blebbing, and fragmentation of apoptotic cells into small membrane vesicles named apoptotic bodies (2–4). These features of apoptosis allow the dead cell to be rapidly and cleanly removed through phagocytosis by neighboring cells and macrophages, and thus the inflammation response is avoided. The critical role of caspases in apoptosis has been demonstrated by genetic studies from *Caenorhabditis elegans* to mouse (5–10).

The first caspase identified, caspase-1, previously known as interleukin-1 β converting enzyme (ICE), processes interleukin-1 β precursor to its mature form. Several unique properties of caspase have been uncovered by the study of caspase-1 (11). True to all functionally characterized caspases, caspase-1 uses a cysteine residue in its active site and is synthesized as an inactive precursor that becomes activated by proteolysis or association with its respective activator molecules (11–13). Caspases cleave substrates after aspartic acid residues, a signature of this group of proteases (11). So far, there are 14 caspases that have been found in mammalian genomes, and they function either during immune response or apoptosis (13).

One of the two best-characterized caspase activation pathways is initiated from mitochondria. In response to apoptotic stimuli, cytochrome *c*, a previously known component of electron transfer chain in mitochondria, gets released to cytosol where it binds to a partner protein Apaf-1 (14, 15). Apaf-1 consists of three functional domains; the N-terminal caspase recruitment domain (CARD), the middle nucleotide-binding and oligomerization domain (NOD), and the C-terminal regulatory region composed of 13 WD-40 repeats (15, 16). This regulatory region normally keeps Apaf-1 in an autoinhibitory state and when cytochrome *c* binds to this region, Apaf-1 becomes activated in the presence of dATP or ATP (17–19). The activation is accomplished through oligomerization of seven individual Apaf-1/cytochrome *c* complexes into a wheel-like heptamer, called apoptosome (16, 19).

The central ring of apoptosome is formed by the conjugation of seven CARD and NOD domains of Apaf-1, and each of the seven spikes extended from the central ring is made of 13 WD-40 repeats bound to one cytochrome *c* (19).

Apaf-1 represents a family of evolutionarily conserved caspase activators. The *Drosophila* DARK/HAC-1/dApaf-1 shares the same domain structure with Apaf-1, and *C. elegans* ced4 shares homology with Apaf-1 with the caspase recruitment and nucleotide-binding and oligomerization (NOD) domains but missing the WD-40 repeats (20–23). A more distantly related protein family consists of the Nod-1 like proteins in mammals and proteins encoded by disease resistance (R) genes in plants (24, 25). These proteins share homology with Apaf-1 in the NOD domain but contain diverse protein–protein interaction domains at their N termini and mostly leucine-rich repeats at their C termini (25). These proteins play an essential role in innate immune response, although their biochemical function has not been fully characterized.

Apaf-1-mediated caspase activation is accomplished through a cascade of caspases, with caspase-9 functioning as the initiator caspase and caspase-3 and caspase-7 as the downstream effector caspases (26). Caspase-9 contains a caspase recruitment domain (CARD) domain of its own at the N terminus through which it binds the central ring of apoptosome (19). Once bound to apoptosome, procaspase-9 becomes activated. The Apaf-1/caspase-9 complex then works as a holoenzyme that cleaves and activates caspase-3 and caspase-7, which in turn cleave their substrates leading to apoptosis (27).

This Apaf-1-mediated caspase activation pathway absolutely requires the presence of dATP or, at higher concentration, ATP (14, 26). However, the precise roles of the nucleotide and cytochrome *c* are still not clear. There is also confusion on whether the binding and/or hydrolysis of nucleotide are needed and, if so, whether it plays a positive or negative role for apoptosome assembly (16, 28, 29). Here we report the detailed biochemical analysis of this caspase-activating pathway addressing the above mentioned unresolved issues.

Materials and Methods

Materials. Nucleotides dATP and dADP were purchased from Amersham Pharmacia; [α - 33 P]dATP was obtained from MP Bioscience. Polyclonal antibodies against Apaf-1, Caspase-9, and Caspase-3 were prepared as described (28).

Production of Proteins. Purified horse cytochrome *c* was prepared as described (14) followed by Mono S chromatography using the SMART system (Amersham Pharmacia). Apaf-1 cDNA was

Conflict of interest statement: No conflicts declared.

Freely available online through the PNAS open access option.

*To whom correspondence should be addressed. E-mail: xwang@biochem.swmed.edu.

© 2005 by The National Academy of Sciences of the USA

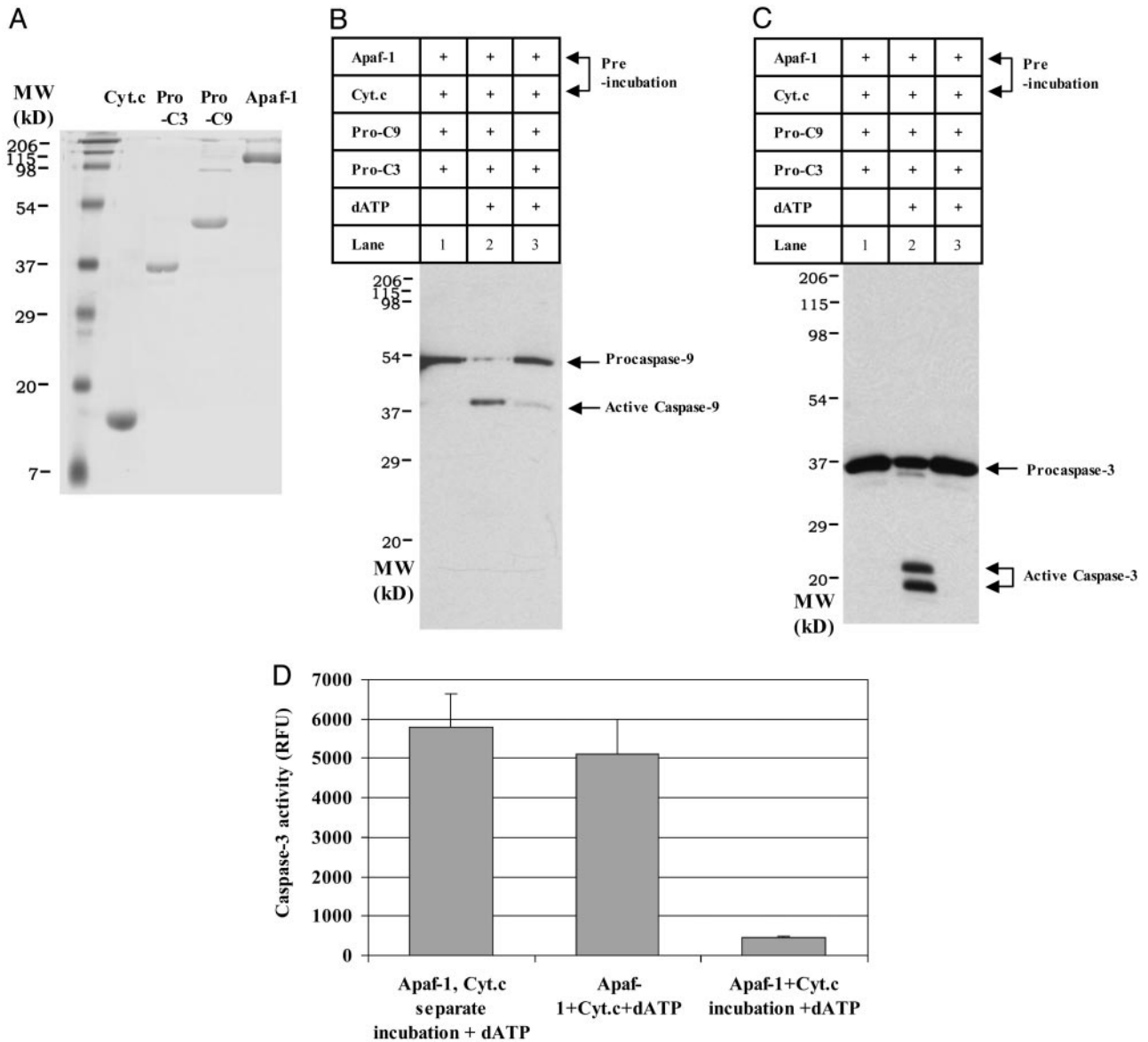


Fig. 1. Apaf-1-mediated caspase activation. (A) Coomassie blue staining of purified horse heart cytochrome c (Cyt.c) and recombinant Apaf-1, pro-caspase-9 (Pro-C9), and pro-caspase-3 (Pro-C3) (1 μ g of protein each). (B and C) Western blot of caspase-9 and caspase-3, respectively. Apaf-1 at a final concentration of 20 nM was incubated with cytochrome c (Cyt.c, 100 nM final concentration), procaspase-9 (Pro-C9), and procaspase-3 (Pro-C3) at a final concentration of 50 nM in the absence or presence of 10 μ M dATP at 30°C for 1.5 h in a final volume of 20 μ l (lanes 1 and 2). In lane 3, Apaf-1 and cytochrome c were preincubated at 30°C for 1 h before the addition of procaspase-9, procaspase-3, and dATP and incubated at 30°C for 1.5 h. The samples were subsequently subjected to SDS/PAGE followed by Western blotting analysis using antibodies against caspase-9 and caspase-3. Cleaved products of procaspase-9 and procaspase-3 are labeled as active caspases. (D) The graph shows the caspase-3 activity measured by fluorogenic caspase-3 substrate. Apaf-1 (20 nM) and cytochrome c (100 nM) were preincubated separately at 30°C for 1 h, then incubated with other components (50 nM procaspase-9, 50 nM procaspase-3, and 10 μ M dATP) at 30°C for 1 h in a final volume of 20 μ l (Left). Apaf-1 and cytochrome c were incubated together with other components at 30°C for 1 h (Center). Apaf-1 and cytochrome c were preincubated together at 30°C for 1 h, then incubated with dATP and other components at 30°C for 1 h (Right). Fluorogenic caspase-3 substrate was added to each sample after the incubation to measure the substrate cleavage as described in *Materials and Methods*.

amplified with oligonucleotides 5'-AGTCGCGGCCGCATG-CACCACCATCATCACCACATGGATGCAAAAAGCTC-GAAATTGTTTGC-3' and 5'-CTTCTCGACAAGCTTGGT-ACCTTAATGATG-3', using full-length Apaf-1 pFastBacI construct (16) as template. A 3.8-kb PCR product was ligated into the pGEM-T Easy vector by using the TA cloning kit (Promega). Plasmid was sequenced and mutations were corrected by using a QuikChange Site-Directed Mutagenesis kit (Stratagene). Corrected Apaf-1 cDNA with six N-terminal histidines and nine C-terminal histidines was then subcloned into NotI/KpnI sites of pFastBacI (Invitrogen). The pFASTBACI

containing the correct Apaf-1 cDNA was then used to make baculovirus, and the recombinant Apaf-1 protein was produced in SF21 cells after infection with the baculovirus according to the manufacturer's instruction. All of the plasmid manipulation and amplification for Apaf-1 were done at <16°C to prevent recombination.

Recombinant Apaf-1 was then expressed and nickel affinity-purified as described (16), followed by Hitrap Q, Heparin, and Superdex 200 chromatography using a fast protein liquid chromatography system (Amersham Pharmacia). Recombinant procaspase-9 and procaspase-3 were expressed and purified as described (28), followed by a Hitrap Q column purification.

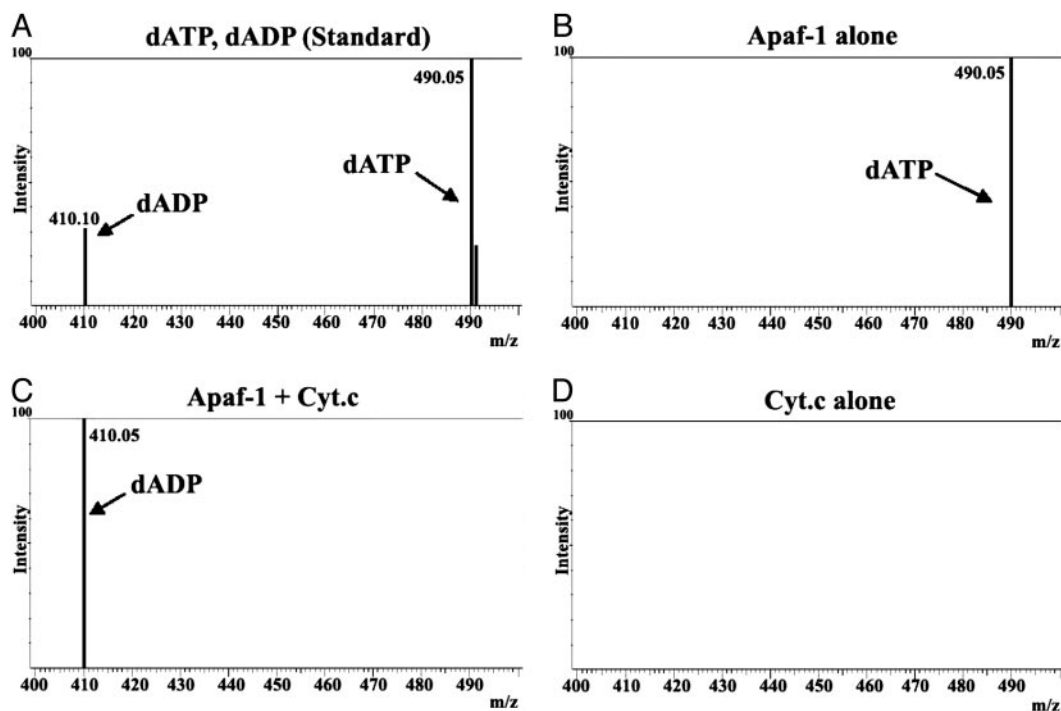


Fig. 2. Apaf-1 is associated with dATP and hydrolyzes it upon cytochrome *c* binding. (A) A mixture of dATP and dADP analyzed by LC-MS. (B) LC-MS analysis of aqueous phase after 40 ng of recombinant Apaf-1 protein was extracted with phenol as described in *Materials and Methods*. A mass peak correlated with dATP was indicated. (C) LC-MS analysis was done as in B, but 40 ng of recombinant Apaf-1 was incubated with 20 ng of cytochrome *c* for 3 h before extraction with phenol. A mass peak correlated with dADP was indicated. (D) LC-MS analysis of aqueous phase after cytochrome *c* alone was extracted with phenol.

Detection of Apaf-1 Bound Nucleotides by LC-MS. Apaf-1 bound nucleotides were analyzed by using a liquid chromatography-mass spectrometry system (LC-MS, Shimadzu). All of the samples were dialyzed at 4°C for 2 h to remove salt and extra nucleotides after incubation of Apaf-1 in the absence or presence of cytochrome *c*. Nucleotides were extracted in the aqueous phase by using phenol/chloroform/isoamyl alcohol (25:24:1, vol/vol, Roche). Samples were then dialyzed against distilled water for 4 h by using dialysis tube with a cutoff molecular mass of 500 Da (Spectrum). The samples were then applied to LC-MS by using ESI polarity switching with column method (1–70% of MeOH/H₂O gradient).

Measurement of dATP Hydrolysis by Apaf-1. The Malachite Green Phosphate Assay kit (POMG-25H, BioAssay Systems) was purchased for measuring dATP hydrolysis. The reaction was carried out in buffer A (20 mM Hepes-KOH, pH 7.5/10 mM KCl/1.5 mM MgCl₂/1 mM EDTA/1 mM EGTA/1 mM DTT/0.1 mM PMSF) containing an additional 5 mM MgCl₂, 35 pmol of Apaf-1, 175 pmol of cytochrome *c*, and other factors as indicated in Fig. 3. Hydrolysis of dATP was measured in a XFluor4 spectrometry reader (Tecan) as instructed in the manual (Bio-Assay Systems)

Glycerol Gradient and Measurement of Apoptosome Activity. Twenty nanograms of purified Apaf-1 and other components indicated in Fig. 4 were incubated at 30°C for 3 h. Samples were then applied onto a 10–30% glycerol gradient in 3.6 ml and centrifuged at 50,000 rpm (256,000 × *g*) at 17°C for 3 h, using SW60Ti rotor (Beckman). Fractions were taken from the top of tube by using a pipette (15 fractions, 240 μl per fraction). Fractions were then used for the Western blotting for Apaf-1 and other assays below.

Apoptosome activity was measured by incubating a 14-μl aliquot of each fraction with 50 nM procaspase-9, 50 nM

procaspase-3, 10 μM dATP, 100 nM cytochrome *c*, and 10 μM fluorogenic DEVD caspase-3 substrate. Samples were transferred to 384-well microplate, and caspase-3 activity was measured by using XFluor4 spectrometry reader (Tecan) (31).

TLC. PEI Cellulose TLC plate was purchased from Selecto Scientific (Suwanee, GA). Active and inactive apoptosome samples were fractionated by Superose 6 chromatography using a SMART system as described (28). A 3-μl aliquot of Apaf-1 peak fraction from each sample was spotted on to the TLC plate and

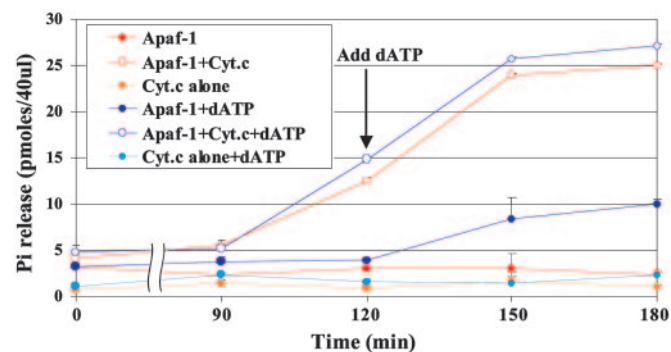


Fig. 3. Cytochrome *c*-stimulated dATP hydrolysis by Apaf-1. Apaf-1 (35 pmol) and cytochrome *c* (175 pmol) were used in a final volume of 40 μl. Aliquots of Apaf-1 alone (filled red circle), Apaf-1 plus cytochrome *c* (open red circle), and cytochrome *c* alone (filled pink circle) were incubated at 30°C for 3 h, and dATP hydrolysis was measured at the indicated time points as described in *Materials and Methods*. For the other three samples, 10 μM of dATP was added to Apaf-1 alone (filled dark blue circle), Apaf-1 plus cytochrome *c* (open dark blue circle), or cytochrome *c* alone (filled light blue circle) 2 h after the starting incubation. The dATP hydrolysis was measured by a Malachite Green Phosphate Assay kit as described in *Materials and Methods*.

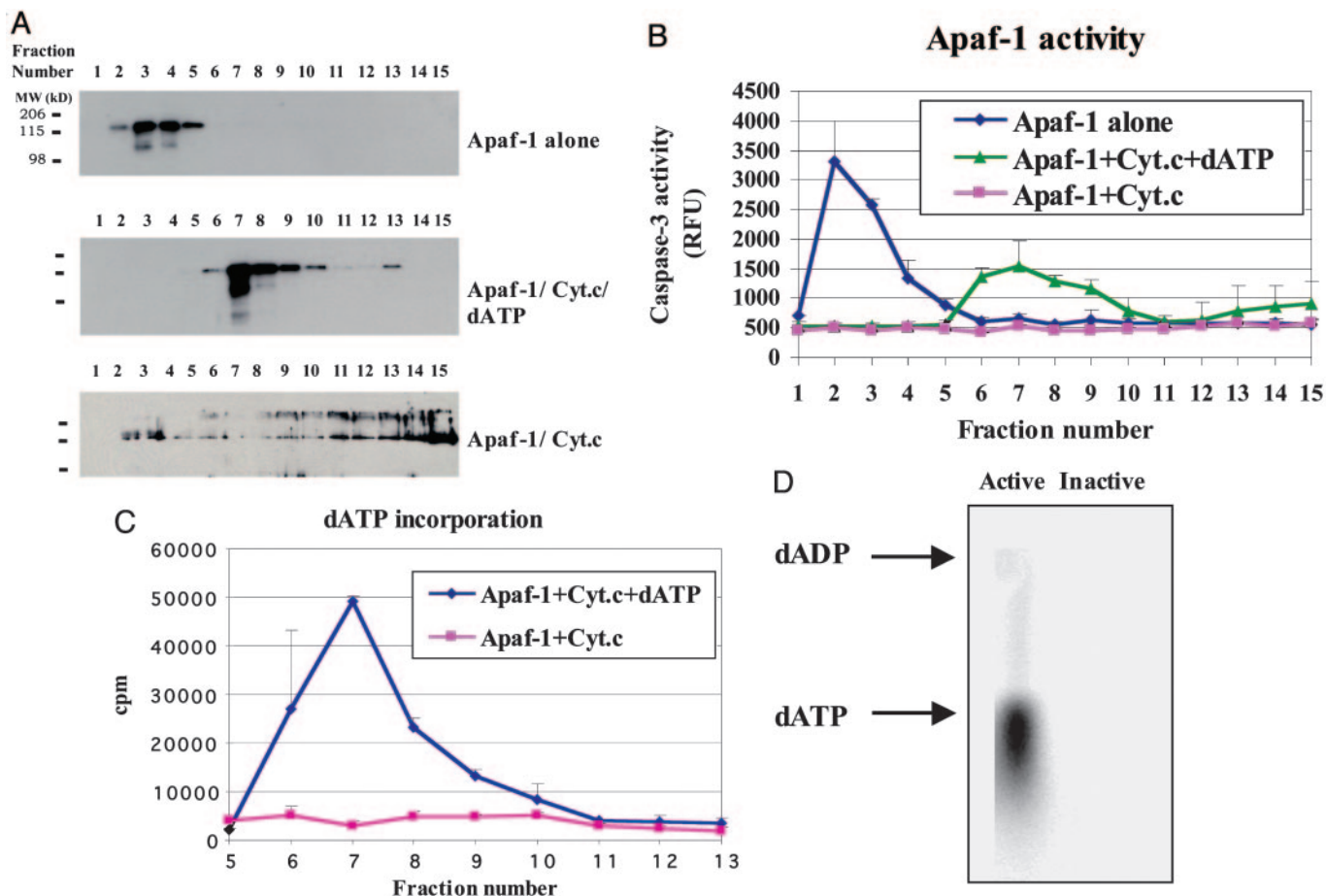


Fig. 4. Apoptosome contains exogenously added dATP. (A) Indicated samples were subjected to glycerol gradient separation after incubation as described in *Materials and Methods*. Fractions from the glycerol gradient were subjected to SDS/PAGE followed by Western blotting using anti-Apaf-1 antibody. (B) The same glycerol gradient fractions as in A were subjected to caspase-3 assay. Aliquots (14 μ l) of glycerol gradient fractions were incubated with 50 nM procaspase-9, 50 nM procaspase-3, 10 μ M dATP, 100 nM cytochrome *c*, and 10 μ M fluorogenic DEVD caspase substrate in a final volume of 20 μ l. Samples were mixed in the test tubes and transferred to 384-well microplates, and caspase-3 activity was measured by using the XFluor4 spectrometry reader (Tecan). (C) dATP incorporation was measured by using [α - 32 P]dATP. A total of 10 μ Ci of [α - 32 P]dATP plus 10 μ M of dATP were incubated with Apaf-1 and cytochrome *c* at 30°C for 3 h (blue diamond). For another sample, 10 μ Ci of [α - 32 P] dATP plus 10 μ M of dATP was added to Apaf-1 and cytochrome *c* mixture after they were preincubated for 1.5 h. The sample was incubated for additional 1.5 h before being subjected to glycerol gradient (pink square). The fractions were then collected as in A, and a 4- μ l aliquot of each fraction was counted for radioactivity by a liquid scintillation counter. (D) For the active apoptosome, 10 ng of Apaf-1, 5 ng of cytochrome *c*, and 10 μ Ci of [α - 32 P]dATP plus 10 μ M of dATP were incubated at 30°C for 3 h before being subjected to a Superpose 6 chromatography column as described in *Materials and Methods*. For the inactive apoptosome sample, 10 ng of Apaf-1 and 5 ng of cytochrome *c* were preincubated at 30°C for 1.5 h. Then, 10 μ Ci of [α - 32 P]dATP plus 10 μ M of dATP were added to the sample, and incubation was continued for 1.5 h before the sample was subjected to the Superpose 6 gel-filtration column. An aliquot of 3 μ l of peak Apaf-1 fraction was spotted on a TLC plate and analyzed as described in *Materials and Methods*.

separated in the separation buffer (1 M formic acid/0.5 M LiCl). The TLC plate was dried and exposed to BAS-IIIIs plate (Fuji) and visualized by Typhoon PhosphorImager and IMAGEQUANT software (Molecular Dynamics).

Results

Reconstitution of Caspase-3 Activation Using Purified Protein Components. As shown in Fig. 1A, we have generated and purified recombinant human Apaf-1, procaspase-9, and procaspase-3 from insect cells by using baculovirus expression system. It is worth mentioning that although we were able to generate recombinant Apaf-1 before, we did it with a pool of Apaf-1 cDNAs instead of a clone (15); we had to use this method because the 13 WD-40 repeat sequences at the 3' end of Apaf-1-coding region were prone to recombination when the plasmid was replicated in bacteria. Therefore, the plasmid prepared from bacteria grown from a single colony was always a mixture resulted from DNA recombination. To circumvent this problem, we pooled bacterial colonies soon after they appeared

on agar plates to minimize the time for recombination. However, after several rounds of propagation, the baculovirus vector containing Apaf-1 cDNA became heterogeneous, and the protein yield was poor. We noted that recombination did not happen if we kept the bacteria-hosting Apaf-1 encoding plasmid under 16°C at all time. We then used this strategy to reclone Apaf-1 ORF, correct all of the mutations, and use it for making Apaf-1 protein in SF21 insect cells. Now, we routinely make up to \approx 10 mg of purified Apaf-1 protein from a liter of SF21 cell culture, and the purified protein was used throughout this study.

As shown in Fig. 1B and C, when purified Apaf-1, procaspase-9, procaspase-3, and cytochrome *c* were mixed in the absence of nucleotide, there was no caspase-9 and caspase-3 activation as measured by their cleavage (lane 1). In contrast, in the presence of 10 μ M dATP, most of caspase-9 and caspase-3 were activated after incubation (lane 2).

Preincubation of Apaf-1 and Cytochrome *c* Without dATP Inactivates Apaf-1. The nucleotide requirement was observed early for cytochrome *c*-induced caspase-3 activation (14). However, sur-

prisingly, when Apaf-1 and cytochrome *c* were preincubated without dATP, they became permanently inactivated, and subsequent addition of dATP was not able to recover the activity (Fig. 1 *B* and *C*, lane 3). On the other hand, preincubating Apaf-1 and cytochrome *c* separately did not affect their activity at all (Fig. 1 *D*). This finding indicated that Apaf-1 underwent irreversible changes when incubated with cytochrome *c* in the absence of dATP.

Other than dATP, ATP is able to support Apaf-1/cytochrome *c*-mediated caspase activation when used at higher concentrations (26, 28). Moreover, the 5'-triphosphate metabolite of clinically used chemotherapeutic drugs 2-chloro-2'-deoxyadenosine (2CdA, cladribine) and 9-β-D-arabino-furanosyl-2-fluoroadenine (fludarabine) can also substitute dATP to activate Apaf-1 (30). On the other hand, other nucleotides including CTP, dCTP, GTP, dGTP, TTP, and UTP are not able to support Apaf-1 function (14).

Apaf-1 Contains a dATP Cofactor. Although ATP is much weaker in activating Apaf-1 than dATP, the cellular concentration of ATP is much higher than dATP. Therefore, it is unclear which nucleotide will be preferably used *in vivo*. Because the nucleotide-binding domain of Apaf-1 is closer to the N terminus than the WD-40 repeat region that may negatively regulate nucleotide binding, we hypothesized that Apaf-1 synthesized in cells might already contain a nucleotide cofactor. The identity of this bound nucleotide may give us a clue about which nucleotide is really used in cells.

The ability to make a large quantity of Apaf-1 recombinant protein in insect cells allowed us to directly examine this scenario. We first denatured purified Apaf-1 by phenol extraction, and then analyzed the aqueous phase in a liquid chromatography-mass spectrometry system (LC-MS). As shown in Fig. 2, a peak that matched the mass of dATP standard was observed when the small molecule associated with Apaf-1 was analyzed by LC-MS (Fig. 2 *A* and *B*). No ATP or dADP was observed under the same extraction and analysis condition, indicating that Apaf-1 indeed contains a dATP cofactor. The dATP bound to Apaf-1 is stable because we did not see any dADP even after we incubated Apaf-1 alone *in vitro* for 3 h (data not shown).

Cytochrome *c* Induces dATP Hydrolysis. Because Apaf-1 activity is triggered by cytochrome *c*, we checked the status of the dATP that bound to Apaf-1 after incubation with cytochrome *c*. As shown in Fig. 2 *C*, we noticed the dATP peak completely disappeared after Apaf-1 was incubated with cytochrome *c* and a new peak correlated with dADP appeared. This finding suggested that cytochrome *c* induces hydrolysis of the Apaf-1-bound dATP to dADP.

To further analyze this hydrolysis event, we used a Malachite Green phosphate assay system that quantitatively measures the released phosphate after incubating purified Apaf-1 with cytochrome *c*. As shown in Fig. 3, there was no phosphate release when Apaf-1, or cytochrome *c* was incubated either alone or with dATP (pink and light blue lines and lines with filled red and dark blue circles). On the other hand, when Apaf-1 was incubated with cytochrome *c* (line with open red circle), the released phosphate was detected after 90-min incubation and the amount increased linearly up to 150 min. The released phosphate reached plateau around 30 pmol, close to the 35 pmol of Apaf-1 protein used in the reaction. Interestingly, the released phosphate remained plateaued at this level even when 10 μM exogenous dATP was added at the linear range of dATP hydrolysis, clearly indicating that dATP is hydrolyzed only once by Apaf-1 (line with open dark blue circle). The exogenously added dATP cannot be further hydrolyzed once one round of dATP hydrolysis is done.

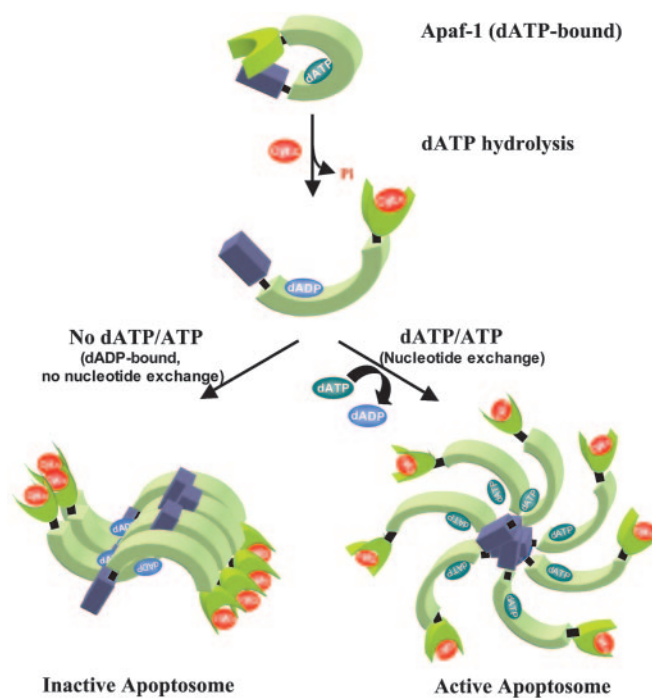


Fig. 5. Model of apoptosome formation. Apaf-1 is associated with dATP. Upon cytochrome *c* binding, Apaf-1 hydrolyzes dATP. If there is extra dATP/ATP, dADP is exchanged with dATP and Apaf-1 forms the active apoptosome. When Apaf-1 is incubated with cytochrome *c* without extra dATP/ATP, dADP-bound Apaf-1 forms the inactive aggregate.

Nucleotide Exchange on Apaf-1 During Apoptosome Formation. How can we explain the requirement of exogenous dATP for apoptosome formation? The logical speculation is that there is a nucleotide exchange step after dATP hydrolysis. Without such an exchange step, Apaf-1 may fold into inactive configuration after the dATP hydrolysis. To further investigate this particular step, we analyzed apoptosome formation by using a glycerol gradient that can separate monomeric Apaf-1 from apoptosome. As shown in Fig. 4 *A*, Apaf-1 alone migrated at fractions 3–4 on top of the gradient but shifted to fractions 6–8 after incubating with cytochrome *c* and dATP, the condition to form apoptosome. The functionality of apoptosome and Apaf-1 was confirmed by adding procaspase-9 and -3 and caspase-3 activity was measured (Fig. 4 *B*). The free Apaf-1 at fractions 3–4 was active in activating caspase-3, and the pre-formed apoptosome peaked at fraction 7 (dark and light blue lines, respectively). In contrast, if Apaf-1 was preincubated with cytochrome *c* in the absence of dATP, Apaf-1 protein formed aggregates that migrated to the bottom of the gradient (Fig. 4 *A* Lower) and showed no caspase-3 activity even when procaspase-9 and -3 were added later (Fig. 4 *B*, red line).

To confirm that there has to be a nucleotide exchange to form functional apoptosome, we added radioactive dATP to the apoptosome-forming reaction and isolated the apoptosome afterward by glycerol gradient. We then measured where the radioactive dATP went by liquid scintillation counting. As shown in Fig. 4 *C*, the radioactive peak was correlated perfectly with that of apoptosome (peak at fraction 7). There was no radioactivity associated with monomeric Apaf-1 or aggregated Apaf-1, indicating that the nucleotide exchange only happens during apoptosome formation. To confirm the identity of the radioactive nucleotide associated with apoptosome, we formed and isolated apoptosome by using radio-labeled dATP. We then analyzed apoptosome-associated radioactivity with TLC. As shown in Fig. 4 *D*, the radioactive nucleotide was confirmed by TLC as exclusively dATP.

Discussion

The above experiments revealed several previously unknown steps during apoptosome formation. As shown schematically in Fig. 5, Apaf-1 generated in insect cells contains dATP as a cofactor. The bound dATP then undergoes one round of hydrolysis to dADP, a process that is stimulated by cytochrome *c*. This hydrolysis appears to serve two roles: (i) it provides energy for the conformational change need for Apaf-1 to transient from the inactive monomeric state to the oligomeric state; and (ii) it allows exogenous dATP (or ATP) to exchange for the dADP that has lower binding affinity for Apaf-1, a critical step for Apaf-1 to form functional apoptosome rather than nonfunctional aggregates. This hydrolysis only happens in one round. Exogenously added dATP will then bind Apaf-1, but remains unhydrolyzed during apoptosome formation.

The formation of the nonfunctional Apaf-1 aggregate is also induced by cytochrome *c* binding to Apaf-1. We actually reisolated cytochrome *c* as an inhibitor of Apaf-1 activity when dATP or ATP was not included in the caspase-3-activating reaction (M.F. and X.W., data not shown). Such aggregates may be identical to the large, inactive Apaf-1 complex first observed in human monocytic tumor cells (31).

Interestingly, the crystal structure of a WD-40-truncated Apaf-1 revealed Apaf-1 in an inactive configuration with an ADP bound to it (29). Because WD-40 repeats serve as an autoinhibitory role, Apaf-1 without this region should be active, yet may easily become inactive if the exogenous dATP or ATP level is low. This finding is consistent with previous observation that WD-40-less Apaf-1 is indeed active in promoting procaspase-9/3 activation but is rather unstable and the only stable configuration might be the dADP or ADP binding form (17, 18, 29). It is also interesting that this form of Apaf-1 expressed in bacteria contains an ADP but not dADP, whereas full-length Apaf-1 expressed in insect cells contains exclusively dATP. The measured difference between dATP and ATP in

binding affinity to Apaf-1 is ≈ 10 -fold, not enough to explain this exclusive binding of dATP because intracellular ATP level is several orders of magnitude higher than dATP (28). One possibility is that dATP level in *E. coli* is very low. Another possibility could be that mammalian and insect cells contain a dATP-specific loading factor for Apaf-1 that is absent in bacteria. Such a factor could potentially function in conjunction with prothymosin- α and PHAPI, two proteins that regulate apoptosome activity (32).

The role of cytochrome *c* in apoptosome formation also becomes clear through the current study. Upon binding to Apaf-1, cytochrome *c* releases the autoinhibition imposed by the WD-40 repeats and allows Apaf-1 to hydrolyze the bound dATP.

This role of cytochrome *c* also suggests that its simple release from mitochondria and binding to Apaf-1 may not necessarily result in the activation of caspase-9/3. Without exogenous dATP or ATP exchange, cytochrome *c* binding to Apaf-1 will irreversibly deplete the Apaf-1 protein in cells without activating caspases. Consistently, when intracellular ATP is depleted, cells undergo necrosis in response to stimuli that normally induce apoptosis, and when the cellular ATP levels are restored, the response shifts back to apoptosis (33). Therefore, we hypothesize that the nucleotide exchange on Apaf-1 may provide another regulatory step for apoptosis.

The question remains whether endogenous Apaf-1 in mammalian cells also exclusively binds dATP. Addressing this question requires improvement on LC-MS method so that we can identify the nucleotide bound to endogenous Apaf-1 by using much less available material.

We thank Drs. Yigong Shi, Joe Goldstein, and Mike Brown for encouragement and critical reading of this manuscript; Ms. Patricia Hamon in Dr. Patrick Harran's laboratory for help with LC-Mass analysis; and Xinchao Yu and Chris Akey for help with glycerol gradient analysis. The work is supported by National Institutes of Health Grant GMRO1 57158 and Welch Foundation Grant I-1412.

- Alnemri, E. S., Livingston, D. J., Nicholson, D. W., Salvesen, G., Thornberry, N. A., Wong, W. W. & Yuan, J. (1996) *Cell* **87**, 171.
- Wyllie, A. H. (1980) *Nature* **284**, 555–556.
- Wyllie, A. H., Kerr, J. F. & Currie, A. R. (1980) *Int. Rev. Cytol.* **68**, 251–305.
- Wyllie, A. H., Morris, R. G., Smith, A. L. & Dunlop, D. (1984) *J. Pathol.* **142**, 66–77.
- Yuan, J., Shaham, S., Ledoux, S., Ellis, H. M. & Horvitz, H. R. (1993) *Cell* **75**, 641–652.
- Chew, S. K., Akdemir, F., Chen, P., Lu, W. J., Mills, K., Daish, T., Kumar, S., Rodriguez, A. & Abrams, J. M. (2004) *Dev. Cell* **7**, 897–907.
- Daish, T. J., Mills, K., Kumar, S. (2004) *Dev. Cell* **7**, 909–915.
- Kuida, K., Zheng, T. S., Na, S., Kuan, C., Yang, D., Karasuyama, H., Rakic, P. & Flavell, R. A. (1996) *Nature* **384**, 368–372.
- Kuida, K., Haydar, T. F., Kuan, C. Y., Gu, Y., Taya, C., Karasuyama, H., Su, M. S., Rakic, P. & Flavell, R. A. (1998) *Cell* **94**, 325–337.
- Hakem, R., Hakem, A., Duncan, G. S., Henderson, J. T., Woo, M., Soengas, M. S., Elia, A., de la Pompa, J. L., Kagi, D., Khoo, W., et al. (1998) *Cell* **94**, 339–352.
- Thornberry, N. A., Bull, H. G., Calaycay, J. R., Chapman, K. T., Howard, A. D., Kostura, M. J., Miller, D. K., Molineaux, S. M., Weidner, J. R., Aunins, J., et al. (1992) *Nature* **356**, 768–774.
- Thornberry, N. A. & Lazebnik, Y. (1998) *Science* **281**, 1312–1316.
- Shi, Y. (2002) *Mol. Cell* **9**, 459–470.
- Liu, X. S., Kim, C. N., Yang, J., Jemmerson, R. & Wang, X. (1996) *Cell* **86**, 147–157.
- Zou, H., Henzel, W. J., Liu, X., Lutschg, A. & Wang, X. (1997) *Cell* **90**, 405–413.
- Zou, H., Li, Y., Liu, X. & Wang, X. (1999) *J. Biol. Chem.* **274**, 11549–11556.
- Srinivasula, S. M., Ahmad, M., Fernandes-Alnemri, T. & Alnemri, E. S. (1998) *Mol. Cell* **1**, 949–957.
- Adrain, C., Slee, E. A., Harte, M. T. & Martin, S. J. (1999) *J. Biol. Chem.* **274**, 20855–20860.
- Acehan, D., Jiang, X., Morgan, D. G., Heuser, J. E., Wang, X. & Akey, C. W. (2002) *Mol. Cell* **9**, 423–432.
- Rodriguez, A., Oliver, H., Zou, H., Chen, P., Wang, X. & Abrams, J. M. (1999) *Nat. Cell Biol.* **1**, 272–279.
- Kanuka, H., Sawamoto, K., Inohara, N., Matsuno, K., Okano, H. & Miura, M. (1999) *Mol. Cell* **4**, 757–769.
- Zhou, L., Song, Z., Tittel, J. & Steller, H. (1999) *Mol. Cell* **4**, 745–755.
- Yuan, J.-Y. & Horvitz, R. H. (1992) *Development (Cambridge, U.K.)* **116**, 309–320.
- Martinon, F., Burns, K. & Tschopp, J. (2002) *Mol. Cell* **10**, 417–426.
- Inohara, N., Ogura, Y. & Nunez, G. (2002) *Curr. Opin. Microbiol.* **5**, 76–80.
- Li, P., Nijhawan, D., Budihardjo, I., Srinivasula, S. M., Ahmad, M., Alnemri, E. S. & Wang, X. (1997) *Cell* **91**, 479–489.
- Rodriguez, J. & Lazebnik, Y. (1999) *Genes Dev.* **13**, 3179–3184.
- Jiang, X. & Wang, X. (2000) *J. Biol. Chem.* **275**, 31199–203.
- Riedl, S. J., Li, W., Chao, Y., Schwarzenbacher, R. & Shi, Y. (2005) *Nature* **434**, 926–933.
- Leoni, L. M., Chao, Q., Cottam, H. B., Genini, D., Rosenbach, M., Carrera, C. J., Budihardjo, I., Wang, X. & Carson, D. A. (1998) *Proc. Natl. Acad. Sci. USA* **95**, 9567–9571.
- Cain, K., Bratton, S. B., Langlais, C., Walker, G., Brown, D. G., Sun, X. M. & Cohen, G. M. (2000) *J. Biol. Chem.* **275**, 6067–6070.
- Jiang, X., Kim, H.-E., Shu, H., Zhao, Y., Zhang, H., Kofron, J., Donnelly, J., Burns, D., Ng, S.-C., Rosenberg, A. & Wang, X. (2003) *Science* **299**, 223–226.
- Eguchi, Y., Shimizu, S. & Tsujimoto, Y. (1997) *Cancer Res.* **57**, 1835–1840.